

Molecule-based Weak Ferromagnet with Unique Magnetic Multiphases

Tetsuro Kusamoto, Emiko Fujiwara, and Akiko Kobayashi*

Research Centre for Spectrochemistry, Graduate School of Science, The University of Tokyo,
Hongo, Bunkyo-ku, Tokyo 113-0033

(Received March 25, 2005; CL-050403)

New charge-transfer salt, $[\mathbf{1} \cdot \text{Fe(III)Cl}_4]$ ($\mathbf{1}$ = tetraselenafulvalene-1,3-dithiol-2-one) was prepared and its crystal structure was determined. The magnetic susceptibility measurements of $[\mathbf{1} \cdot \text{Fe(III)Cl}_4]$ suggested not only that $[\mathbf{1} \cdot \text{Fe(III)Cl}_4]$ is a weak ferromagnet but also that $[\mathbf{1} \cdot \text{Fe(III)Cl}_4]$ has several magnetic phases, depending on the applied field at low temperature.

In the past decades, multifunctional magnetic molecular materials consist of charge-transfer salts with planar organic donors¹ or transition-metal complexes,² have been highly focused and investigated. In this system, we can tune their electronic states and physical properties by modifying the donors, ligands and changing the metal ions. Recently, H. Kobayashi et al. have developed the magnetic molecular conductors $(\text{BETS})_2\text{MX}_4$ [BETS = bis(ethylenedithio)tetraselenafulvalene; M = Fe, Ga; X = Cl, Br]^{1a} in which the selenium atoms of the donor, the van der Waals radii of which is larger than those of oxygen and sulfur, play an important role to construct multidimensional electrical states and multifunctional physical properties. Thus, we focused on the novel potential of selenium, and prepared a new donor $\mathbf{1}$ (=tetraselenafulvalene-1,3-dithiol-2-one) as a building block for realizing the hybrid molecule-based materials. Here, we report the synthesis and physical properties of $\mathbf{1}$ -based molecular weak ferromagnet $[\mathbf{1} \cdot \text{Fe(III)Cl}_4]$, which have peculiar magnetic multiphases at low temperature.

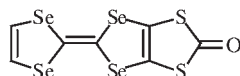


Chart 1. New donor $\mathbf{1}$.

The synthesis for donor $\mathbf{1}$ is as follows. The generated TSF (= tetraselenafulvalene) dithiolate³ in THF/MeOH (v:v = 1:1) was reacted with ZnCl_2 and ${}^n\text{Bu}_4\text{N} \cdot \text{Br}$. The resulting Zn complex was treated with triphosgene in THF at -78°C -r.t. After purification by a column chromatography (deactivated silica gel, eluent: CS_2), Se-containing donor $\mathbf{1}$ was obtained as green crystals in 63% yield.

$[\mathbf{1} \cdot \text{Fe(III)Cl}_4]$ was prepared by electrochemical oxidation of the donor $\mathbf{1}$ with $\text{Et}_4\text{N} \cdot \text{Fe(III)Cl}_4$ in chlorobenzene under a constant voltage of 2.5 V. Black plate crystals of $[\mathbf{1} \cdot \text{Fe(III)Cl}_4]$ grew on the anode within 3 weeks.

The crystal structure of $[\mathbf{1} \cdot \text{Fe(III)Cl}_4]$ was analyzed by single-crystal X-ray diffraction.⁴ In the unit cell, one FeCl_4^- anion and one donor $\mathbf{1}^+$ are crystallographically independent (Figure 1a). Donors form the dimeric structure with head-to-tail overlap mode, in which the two donors are related with inversion center. There are a lot of $\text{Se(S)} \cdots \text{Se(S)}$ contacts not only intradimer but also interdimer, constructing 2D electrical networks parallel to the ac plane, as shown in Figure 1b. Each 2D layer is interlinked by $\text{O} \cdots \text{Se}$ contacts ($3.21(1) \text{ \AA}$) between donors in their layers. As

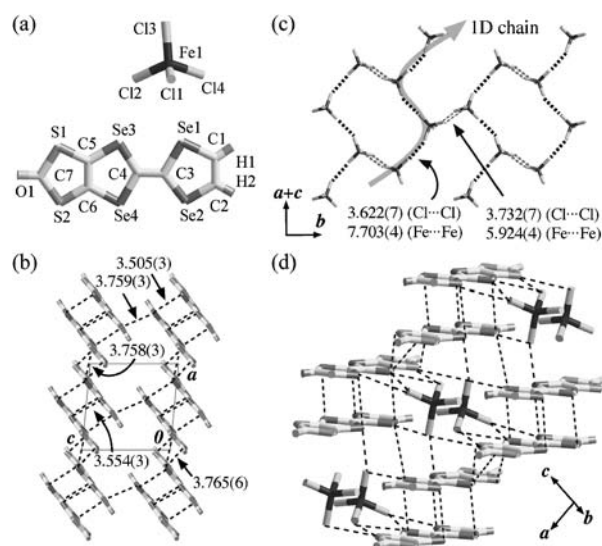


Figure 1. Crystal structure of $[\mathbf{1} \cdot \text{FeCl}_4]$. (a) Crystallographically independent molecules. (b) The sheet structure of the donors projected onto the ac plane. The dotted lines show $\text{Se(S)} \cdots \text{Se(S)}$ contacts (\AA) between donors. (c) The sheet structure of anions projected onto the $(a+c)b$ plane. The dotted lines show short distances (\AA) between anions. (d) The arrangement of donor dimers and anion dimers. The dotted lines show atomic contacts between ions.

shown in Figure 1c and 1d, anions also form the dimeric structure, in which the two anions are related with inversion center. There are short $\text{Cl} \cdots \text{Cl}$ distances between anions, forming a 2D anionic layers parallel to the $(a+c)b$ as shown in Figure 1c where the shortest $\text{Cl} \cdots \text{Cl}$ and $\text{Fe} \cdots \text{Fe}$ distances are presented. The interdimer $\text{Cl} \cdots \text{Cl}$ distances ($3.622(7) \text{ \AA}$) are shorter than those for intradimer ($3.732(7) \text{ \AA}$), indicating that anions construct 1D chains with interchain interaction in the 2D layer. These anion structures reflected the magnetic properties, mentioned below. The shortest $\text{Cl} \cdots \text{Cl}$ and $\text{Fe} \cdots \text{Fe}$ distances for inter-layer are $6.070(7) \text{ \AA}$ and $9.028(4) \text{ \AA}$, respectively. In the crystal, donor 2D layers and anion 2D layers are complexly intercalated, and consequently form the alternate stackings of each dimer along $[\bar{1} 0 1]$ direction (Figure 1d). There are a lot of atomic contacts between anions and donors, which are considered to produce unique physical properties.

The electrical resistivity of this salt approximately along the a axis was measured by conventional four-probe method. The room temperature resistivity of $[\mathbf{1} \cdot \text{Fe(III)Cl}_4]$ was $100 \Omega \cdot \text{cm}$. The temperature dependence of resistivity was semiconductive down to 60 K with an activation energy of 48 meV. Poor conductivity is due to the monocationic state and dimeric structure of the donor.

The static magnetic susceptibility of this salt was measured

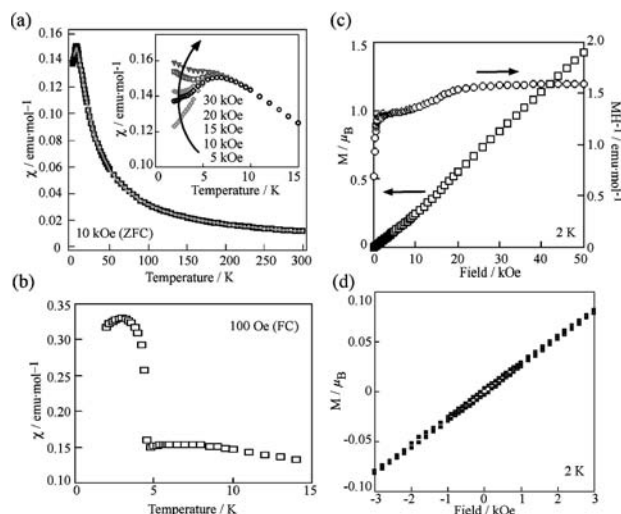


Figure 2. The magnetic properties of $[1\text{-FeCl}_4]$. (a) The temperature dependence of the zero-field-cooled susceptibility under several fields. The line represents the fitting curve of the experimental data to equations 1 and 2. (b) The field-cooled susceptibility at 100 Oe. (c) The field dependence of magnetization at 2 K. (d) The hysteresis loop in the ± 3 kOe at 2 K.

by a SQUID magnetometer using polycrystalline samples under several magnetic fields to investigate the magnetic properties. As shown in Figure 2, the susceptibility under 5 K showed intriguing characteristic behavior, depending on the applied fields. The temperature dependence of the susceptibility above 30 K measured at 10 kOe obeyed the Curie–Weiss law with $C = 3.64 \text{ emu}\cdot\text{K}\cdot\text{mol}^{-1}$ and $\theta = -13.4 \text{ K}$, suggesting the existence of a short-range antiferromagnetic interaction between spins. Obtained C value was lower than 4.375 that we expected for a high-spin state of Fe(III) ion ($S = 5/2$) with $g = 2.00$ and singlet state of dimerized donors. As temperature decreased, the susceptibility of this salt increased, and reached the rounded maximum of $0.15 \text{ emu}\cdot\text{mol}^{-1}$ at 6.5 K, then decreased down to 5 K (Figure 2a). To estimate the magnetic interactions between anions, we applied several spin models, based on the structures of anions (Figure 1c) and measured magnetic data (Figure 2a). The susceptibility above 5 K could be fitted by 1D uniform chain model proposed by Fisher⁵ ($H = -J\sum S_i S_{i+1}$), with introducing the interchain interaction parameter zJ' by mean field approximation.⁶

$$\chi_{\text{chain}} = [Ng^2\mu_B^2 S(S+1)/(3k_B T)] [(1+u)/(1-u)], \quad (1)$$

$$\chi = \chi_{\text{chain}} / [1 - (2zJ'/Ng^2\mu_B^2)\chi_{\text{chain}}], \quad (2)$$

where $u = \coth[2JS(S+1)/k_B T] - k_B T/[2JS(S+1)]$ and $S = 5/2$. The other parameters are the general. From this expression, intrachain interaction J/k_B and interchain interaction zJ'/k_B ($z = 2$) were obtained as -2.57 K and -0.22 K , respectively. These results indicated that antiferromagnetic interactions are dominant in the crystal, and magnitude of the interaction for intrachain is larger than that for interchain.

Below 5 K, the susceptibility of this salt showed field dependence, as shown in Figure 2a. At 5 kOe, it decreased as temperature decreased, and approached a value of $0.11 \text{ emu}\cdot\text{mol}^{-1}$ by extrapolating the temperature to zero. At 5–15 kOe, the susceptibility also decreased corresponding to the strength of the applied field as temperature decreased. This behavior is a typical

character for antiferromagnet, suggesting that the antiferromagnetic (AF) transition occurred at about 5 K under these fields. Furthermore, the magnetic anisotropy, though it was a preliminary result, was also observed at these conditions. Over 20 kOe, the AF ordering was almost overcome by the field, suggesting that spin-flop (SF) occurs between 15 and 20 kOe. However, the field-cooled susceptibility at 100 Oe was quite different from that over 5 kOe. As shown in Figure 2b, susceptibility at 100 Oe first decreased from 6.5 K, then showed abrupt jump at 4.8 K, which finally reached the maximum of $0.33 \text{ emu}\cdot\text{mol}^{-1}$ at 3 K. This value was less than (or was only 0.12% of) that in case the spins were aligned perfectly parallel. These results suggested that the ferromagnetic ordering resulting from spin canting occurred around 4.8 K at 100 Oe. These peculiar magnetic characters were also confirmed by the field dependence of magnetization at 2 K (Figures 2c and 2d).

As the applied field increased from 0 to 50 kOe, the magnetization linearly increased with the inflection point at around 12 and 18 kOe, these are due to the SF transition (Figure 2c). The magnetization only reached a value of $1.43 \mu_B$ even at 50 kOe, which was obviously smaller than the theoretical saturation value of $5 \mu_B$. Furthermore, the hysteric behavior was observed in the range of ± 3 kOe with a coercive field of 100 Oe and small remanent magnetization of $5.38 \times 10^{-4} \mu_B$ ($=15 \text{ emu}\cdot\text{Oe}\cdot\text{mol}^{-1}$, as shown in Figure 2d), suggesting the presence of ferromagnetic ordering due to spin canting. These magnetic results revealed that this salt is a weak-ferromagnet under 100 Oe at 2 K, but it changes to the antiferromagnet when the applied field increases up to 5000 Oe, and antiferromagnetically ordered state is overcome by more stronger external field ($>20 \text{ kOe}$), turning into SF state.

The Dzyaloshinsky–Moriya interaction⁷ is one possible solution to consider the origin of spin canting, but it seems not to be appropriate to this salt because of the presence of inversion center between two anions, which relates to them. In this case, superexchange interaction between anions through π electrons on donors, each of which potentially have $S = 1/2$ spin, may be another possible reason to explain the origin of spin canting and the phase transition from weak-ferromagnetic (WF) state into AF state. To make these peculiar physical properties of this salt clear, the more detailed magnetic and structural investigations at low temperature are needed. In summary, we have developed 1-based molecular weak-ferromagnet $[1\text{-Fe(III)Cl}_4]$ with magnetic multistates (WF state, AF state, SF state, and paramagnetic state). The more precise and detailed investigations for this type of salts, including 1-based GaCl_4^- salt, are now in progress.

References and Notes

- 1 a) H. Kobayashi, H. B. Cui, and A. Kobayashi, *Chem. Rev.*, **104**, 5265 (2004). b) T. Enoki and A. Miyazaki, *Chem. Rev.*, **104**, 5449 (2004).
- 2 a) A. Kobayashi, E. Fujiwara, and H. Kobayashi, *Chem. Rev.*, **104**, 5243 (2004). b) R. Kato, *Chem. Rev.*, **104**, 5319 (2004).
- 3 K. Takimiya, Y. Kataoka, N. Nishihara, Y. Aso, and T. Otsubo, *J. Org. Chem.*, **68**, 5217 (2003).
- 4 Crystal data for $[1\text{-FeCl}_4]$: fw = 679.71, monoclinic, $P2_1/n$, $a = 9.028(8)$, $b = 19.90(2)$, $c = 9.241(9) \text{ \AA}$, $\beta = 95.611(5)^\circ$, $V = 1652(3) \text{ \AA}^3$, $Z = 4$, $D_{\text{calcd}} = 2.73 \text{ g}\cdot\text{cm}^{-3}$, 4420 unique reflections, the final R and R_w were 0.037 and 0.049 (2070 reflections [$I > 2.0\sigma(I)$]).
- 5 a) M. E. Fisher, *Am. J. Physiol.*, **32**, 343 (1964). b) G. R. Wagner and S. A. Friedberg, *Phys. Lett.*, **9**, 11 (1964).
- 6 C. J. O'Connor, *Prog. Inorg. Chem.*, **29**, 203 (1982).
- 7 a) I. Dzyaloshinsky, *J. Phys. Chem. Solids*, **4**, 241 (1958). b) T. Moriya, *Phys. Rev.*, **120**, 91 (1960).